Electrodeposition of chitosan enables synthesis of copper/carbon composites for H_2O_2 sensing

M. Islam [a, *], N. Arya [a, b], P.G. Weidler [c], J.G. Korvink [a], V. Badilita [a, **]

[a] Institute of Microstructure Technology, Karlsruhe Institute of Technology, Hermann-von-Helmholtz-Platz 1, 76344, Eggenstein-Leopoldshafen, Germany
[b] Department of Chemical and Energy Engineering, Otto von Guericke University Magdeburg, Universitat Platz 2, 39106, Magdeburg, Germany
[c] Institute of Functional Interfaces, Karlsruhe Institute of Technology, Hermann-von-Helmholtz-Platz 1, 76344, Eggenstein-Leopoldshafen, Germany

ARTICLE INFO

Keywords:
Electrochemical deposition
Biopolymer derived carbon
Metal/carbon composite
Carbonization
Biosensor

ABSTRACT

This work presents a novel approach in synthesizing copper (Cu)/carbon composite materials by electrodeposition of the biopolymer chitosan, a renewable carbon precursor, on a copper anode, followed by pyrolysis of the electrodeposited chitosan gel. The amount of copper in the Cu/carbon composite material can be controlled by modifying the pH of the chitosan solution from which the electrodeposition is performed. This further influences the physical properties of the composite material. Here we show a 14 fold increase in electrical conductivity of the Cu/carbon composite, when compared to the material without copper inclusions. Metal/carbon composite materials have a wide range of applications already reported in the literature. As a proof of concept, we demonstrate the electrochemical sensing capability of this Cu/carbon material for non enzymatic detection of hydrogen peroxide, achieving a sensitivity of 58.9 μA/mM cm^2, which is comparable to state of the art non enzymatic hydrogen peroxide sensors. The anodic electrodeposition of chitosan proves to be a simple and straightforward medium for synthesis of Cu/carbon composites. We speculate that this method can be extended to obtain other metal/carbon composites as a low cost alternative for the fabrication of functional composite electrodes.

1. Introduction

Metal/carbon composites are an interesting class of materials due to their unique properties, such as high electrical conductivity, high wear resistance, and adjustable electrochemical properties. These properties have enabled the use of metal/carbon composites in a variety of applications, for instance as coating material, or as electrodes in energy devices and biosensors [1–5]. The preparation of metal/carbon composites includes deposition of metal on carbon surfaces [6,7], and carbonization of a precursor composite [3,8,9]. Deposition methods, such as sputtering and microwave plasma enhanced chemical vapor deposition, involve sophisticated infrastructure, which makes the preparation process complex and expensive. Furthermore, deposition methods can only enable metal incorporation on the surface of the carbon material. In comparison, infiltration of a metal salt in a carbon precursor allows for a simpler method for synthesis of the metal/carbon composite. However, selection of the precursors often becomes a crucial factor in this process, which can require a long sample preparation time. Furthermore, many metal precursors are highly corrosive, which requires additional sample handling precautions. In recent years, metal organic frameworks (MOFs) have emerged as a novel material for the preparation of metal/carbon composite through one step carbonization [1,10]. This comes with the disadvantage that the synthesis of MOFs is an extremely slow process, and requires a complex chemical process. Furthermore, the carbon precursors which are used in most of these processes are mainly petroleum derived and non renewable.

In this work, we propose the electrodeposition of chitosan on copper electrodes as a sustainable and environmentally friendly medium to prepare metal/carbon composite materials. Chitosan is a derivative polysaccharide from chitin, which is the second most abundant biopolymer in nature after cellulose [11,12]. Chitosan has proven to be a reliable candidate for the synthesis of carbon material upon carbonization in various applications. For example, Deng et al. reviewed the use of chitosan as a biomass precursor for synthesis of nitrogen doped carbon in supercapacitor applications [13]. Peng et al. synthesized mesoporous carbon material by

* Corresponding author.
** Corresponding author.
E-mail addresses: monsur.islam@kit.edu (M. Islam), vlad.badilita@kit.edu (V. Badilita).

carbonization of a chitosan film in nitrogen environment for selective carbon dioxide (CO_2) capture from dilute industrial sources [14]. Guo et al. synthesized 3D hierarchical N doped carbon nanoflowers using chitosan as the carbon precursor in a silica template approach, which showed superior performance as electrode in lithium sulphur batteries [15]. Chitosan also shows pH dependent solubility, which has enabled the patterning of chitosan on various surfaces using electrodeposition [16–20]. Electrodeposition is advantageous for patterning chitosan, because it allows for both temporal and spatial control of multiple layers of chitosan film on the electrode surface [21], which has enabled the deposition of chitosan films on a variety of microdevice geometries. For example, Wu et al. reported the electrodeposition of chitosan on microfabricated gold electrodes as thin as 20 μm [22]. A member of the present team of authors previously demonstrated electrodeposition of chitosan on the vertical sidewall of an integrated SU 8 microfluidic channel to operate as a chitosan mediated DNA hybridization biosensor [23,24]. Electrodeposition further allows for the deposition of metal/chitosan composite films by adding a metal precursor in the polyelectrolyte mix. For example, Ma et al. fabricated an immunosensor by electrodeposition of gold nanoparticle/chitosan composite for determination of aflatoxin B1 in maize. The gold nanoparticle/chitosan was achieved by mixing chloroauric acid, a gold precursor, in the chitosan solution during electrodeposition [25]. Pang and Zhitomirsky demonstrated the deposition of silver/chitosan composites through addition of silver nitrate in the chitosan solution during electrodeposition [26]. Towards deposition of composite films, Geng et al. reported that it is possible to obtain metal/chitosan composites without adding any metal precursor in the chitosan solution. They demonstrated that the chitosan molecules coordinated with the metal ions generated from the electrode within the polyelectrolyte, and deposited on the anode surface at a specific pH of the polyelectrolyte [19]. Such metal ion mediated electrodeposition enables a simple and fast approach for fabricating metal/chitosan composite. Here, we postulate that the pyrolysis of such metal/chitosan composite can lead to a simple and fast medium for the synthesis of a metal/carbon composite, and simpler when compared to the methods mentioned earlier.

In this work, we demonstrate the synthesis of a copper (Cu)/carbon composite material using metal ion mediated electrodeposition of chitosan, followed by carbonization in an inert atmosphere. We study how the pH of the polyelectrolyte solution used during electrodeposition can control the amount of Cu in the Cu/carbon composite. The morphology of the Cu in the composites also shows a strong dependence on the pH of the polyelectrolyte. The Cu/carbon composites show significant improvement in their electrical conductivity compared to the native carbon material. Utilizing the excellent biocatalytic properties of Cu [27,28], we further demonstrate the amperometric biosensing capabilities of the Cu/carbon composite synthesized here. The Cu/carbon composite shows good sensitivity for non enzymatic detection of hydrogen peroxide (H_2O_2), and is comparable in performance to other non enzymatic amperometric biosensors.

2. Results and discussion

2.1. Electrodeposition of chitosan

We performed electrodeposition of chitosan using polyelectrolyte solution featuring different pH values ranging from 2 to 6, and copper electrodes, both as cathode and anode, using a set up schematically illustrated in Fig. 1. The highest pH we were able to use for electrodeposition was 6. A pH value higher than 6 makes the chitosan insoluble in the aqueous solution, which is not suitable for

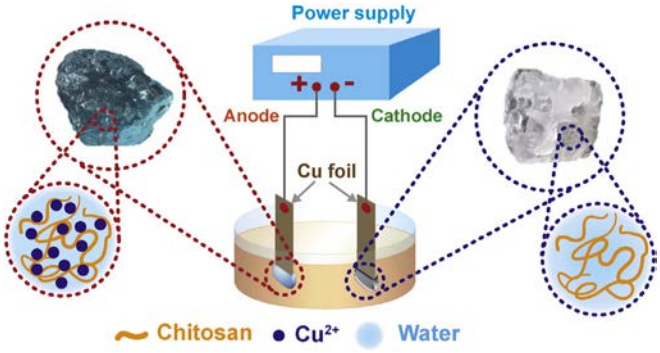

Fig. 1. Illustration of the set up for electrodeposition of chitosan. Copper foils are used for both cathode and anode. The electrodeposited gels on cathode and anode are shown. The cathodic gel appears white, whereas anodic gel appears blue. The blue color of the anodic gel is attributed to the presence of Cu^{2+} ions in the chitosan matrix. The compositions of the cathodic and anodic gel are illustrated as well.

electrodeposition [18,29]. For the pH values ranging from 2 to 6, stable chitosan hydrogels were obtained on the cathode. This was due to the fact that the amino ($-NH_2$) groups present in chitosan solution were protonated in the acidic media, and chitosan particles near the cathode surface experienced relatively high pH, which made the chitosan particles insoluble at the electrode interface, resulting in deposition of the chitosan on the cathode surface [29,30]. No anodic deposition was observed, when using a polyelectrolyte with a pH below 5. However, a thick and stable anodic hydrogel started to appear on the anode when the pH was 5 and above. In contrast to the white cathodic hydrogel, the anodic gel appeared to be blue, as shown in Fig. 1 and S1. The blue color of the anodic hydrogel was attributed to Cu^{2+} ions in aqueous solution. This was in agreement with the article published by Geng et al. [19]. They reported that the anodic copper electrode generates Cu^{2+} ions because of electrochemical oxidation during electrodeposition. The chitosan molecules adjacent to the anodic surface coordinate with the Cu^{2+} ions through chelation and deposit on the anode surface as a stable hydrogel. Anodic deposition of chitosan has been previously reported by, e.g., Gray et al. [31]. However, in the work of Gray et al. anodic deposition occurred due to partial oxidation of the chitosan molecules, which generated aldehydes and coupled covalently with the amine groups. Furthermore, they showed that in a chitosan solution containing HCl, a pH gradient appeared near the anode during electrodeposition. The pH gradient can reach a pH of 1.0 at the vicinity of the anode surface. Such low pH is not suitable for chelation of chitosan with metal ions [32], and did not apply to our experiment. It should be mentioned here that Gray et al. used a gold electrode for electrodeposition and did not achieve any anodic deposition in the solution containing HCl [31]. The anodic deposition only occurred in the solution containing acetic acid. However, the anodic gel did not feature any metal ions. Our hypothesis is that the anodic deposition of a metal/chitosan composite hydrogel depends on the choice of electrode material as well as the choice of acid used to prepare the chitosan solution. An extensive study is needed to characterize the influence of different experimental parameters, i.e., choice of metal electrodes and choice of acid to form the acidic solution, and thereby explore in depth the mechanism of the anodic deposition of metal/chitosan composite gel.

2.2. Composition of carbonized gel

We carbonized the hydrogels electrodeposited on the anodic surfaces, which were obtained at a pH of 5 and higher. The

carbonization was carried out in a nitrogen environment at 900 °C with a heating rate of 5 °C/min. For comparison, we chose a cathodic hydrogel sample obtained at pH value of 2 and subjected this sample to a similar heating protocol. The carbonized anodic samples featured a brown color, whereas the cathodic sample appeared to be black, as shown in Fig. S2. We performed X ray diffraction (XRD) of the carbonized samples to investigate the composition and crystalline structure of the materials. The XRD patterns of the carbonized samples are presented in Fig. 2a. The XRD pattern for the cathodic gel exhibited two broad peaks around 2θ 26° and 2θ 44°, which were indexed to (002) and (100)/(101) reflections of carbon, respectively, according to the International Centre for Diffraction Data (ICDD) PDF number 25 0284. Such reflections are characteristics of amorphous carbon [33,34]. This was in accordance with previous publications reporting synthesis of carbon from pyrolysis of chitosan [35,36]. Tiny peaks corresponding to accidental contamination with Na_2CO_3 (ICDD PDF number 18 1208) were also observed in the XRD pattern for the carbonized sample stemming from the cathodic deposition from the solution with a pH value of 2. The analysis at the elemental level of the cathodic carbon sample is presented in Fig. S4c.

The XRD diffractograms for anodic samples obtained from solutions at pH 5, 5.5 and 6 exhibited distinct peaks for Cu at 2θ of 43.2°, 50.4° and 74.1°, which were indexed to (111), (200) and (220) crystalline planes, respectively, and matched to ICDD PDF no: 04 0836. Furthermore, broad peaks around 2θ 26° and 2θ 44° were also observed (see Fig. S3a), similar to the peaks observed for pH 2, confirming the presence of a significant amount of amorphous carbon in these samples. Therefore, the XRD patterns for the carbonized anodic samples confirmed the formation of Cu/carbon composites through carbonization of the anodic chitosan hydrogels. We further calculated the crystallite size of the Cu particles obtained for different pH values using the Scherrer equation and plotted in Fig. S3b. The crystallite size increased from 28.6 ± 1.0 nm for the sample obtained from the solution with the pH value of 5−31.3 ± 2.2 nm for the sample obtained from the solution with the pH value of 6. We hypothesized that increasing the pH of the chitosan solution might have resulted in a higher amount of Cu^{2+} in the anodic gel. During carbonization, the Cu^{2+} ions sintered together to form crystallites in a carbon matrix. Higher amount of Cu^{2+} ions in the gel might have yielded a larger crystallite size during the carbonization process. The pH dependence of the Cu^{2+}

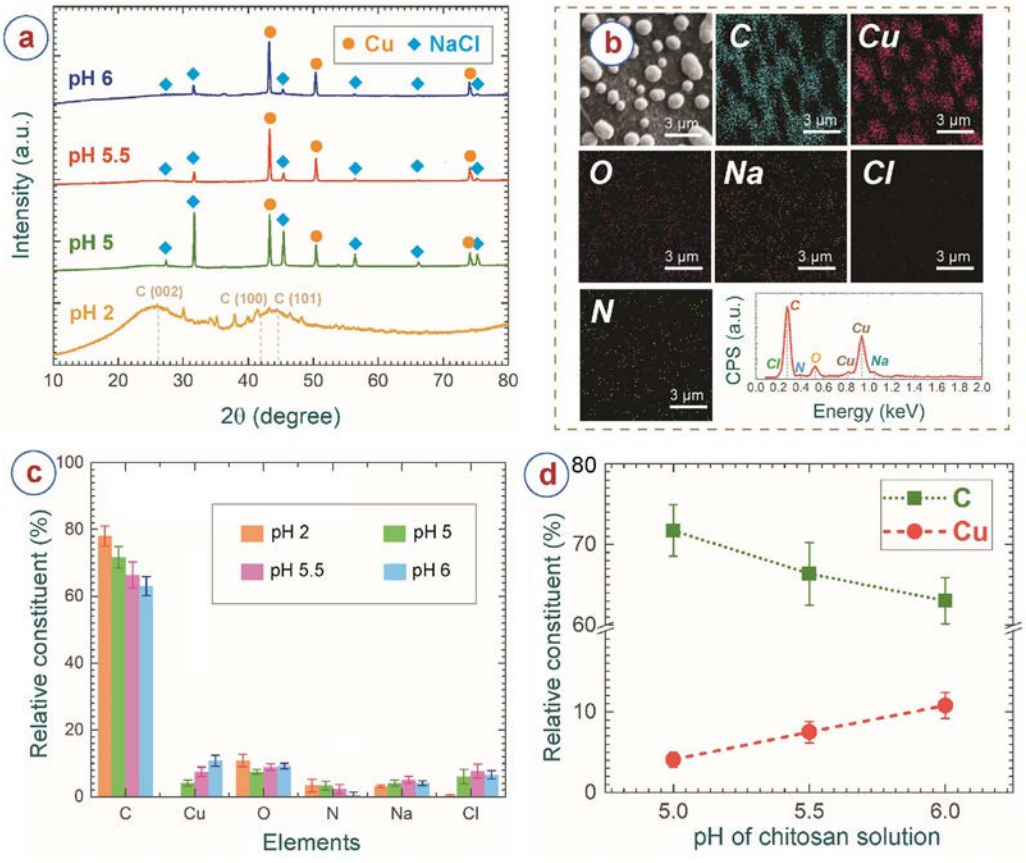

Fig. 2. (a) XRD pattern of the carbonized electrodeposited samples obtained at different pH. Sample of pH2 was electrodeposited on the cathode, other samples were obtained by anodic electrodeposition. The electrodeposited samples were carbonized at 900 °C in nitrogen environment using a heating rate of 5 °C/min. Example of (b) EDX mapping of a carbonized anodic gel showing the presence of carbon (C), copper (Cu), oxygen (O), sodium (Na), chlorine (Cl) and nitrogen (N), and corresponding diffraction pattern confirming presence of these elements. This particular example was for the sample obtained for pH 6. (c) Relative elemental constituent in percentage present in the carbonized anodic gel obtained at different pH values, calculated using the EDX result of each sample. For comparison, results for the carbonized cathodic gel obtained at pH 2 are also plotted. (d) Effect of pH on the amount of copper and carbon for the anodic samples. EDX was performed at minimum six spots on the sample for each pH. Each data point represents average value of the measurements and error bar represents the standard deviation in measurement.

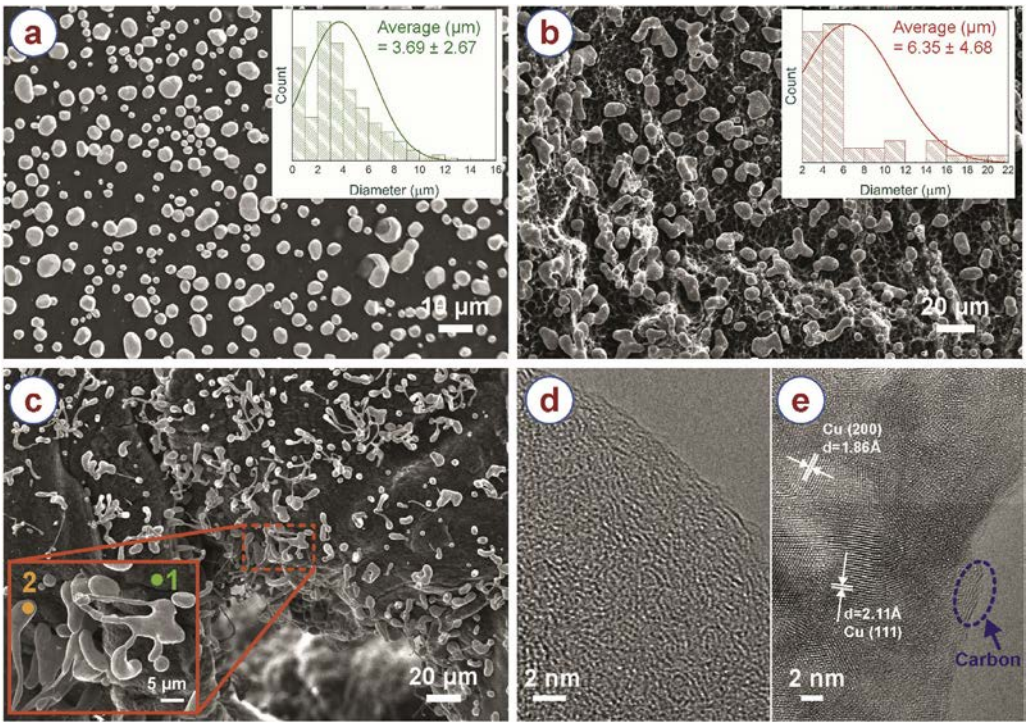

Fig. 3. SEM images of carbonized anodic gel obtained at (a) pH 5, (b) pH 5.5 and (c) pH 6. Insets of (a) and (b) show the Cu particle size distribution of the gel for pH 5 and pH 5.5, respectively. Inset of (c) shows high magnification SEM of the carbonized gel at pH 6, showing irregular and larger particle size. HRTEM image of (d) spot 1, and (e) spot 2 as indicated in the inset of (c).

amount in the anodic gel was confirmed by energy dispersive X ray (EDX) analysis. Along with the Cu peaks, several other peaks were also observed in the XRD patterns for the anodic samples, which were attributed to sodium chloride (NaCl) (ICDD PDF No: 05 0628). NaCl was formed as a reaction product between the NaOH which was added to the chitosan solution for pH adjustment and the HCl used to dissolve the chitosan powder. NaCl was trapped inside the anodic gel matrix and remained in the Cu/carbon composite after the carbonization process.

Elemental analysis of the carbonized gels was performed using EDX. The EDX mapping and the EDX pattern (Fig. 2b) of a carbon ized anodic gel confirmed the presence of the elements carbon (C), copper (Cu), oxygen (O), sodium (Na), chlorine (Cl) and nitrogen (N). Fig. 2c shows the amount of different elements present in the carbonized samples for various pH values. Carbon remained the major component in the sample. However, the amount of carbon in the carbonized anodic samples was lower than that of the cathodic gel. This was expected as no copper particles were present in the cathodic sample. Among the anodic samples, a dependence of pH on the amount of carbon and copper was observed from the EDX results (Fig. 2d). The amount of carbon decreased from 71.7 ± 3.2% for the sample corresponding to the pH 5 solution to 63.0 ± 2.8% for the sample corresponding to pH 6 solution, whereas the amount of copper increased from 4.1 ± 0.9% for the sample corresponding to pH 5 solution to 10.8 ± 1.6% for the sample corresponding to pH 6 solution. This confirms the earlier hypothesis that higher pH of the chitosan solution resulted in higher amount of Cu^{2+} in the anodic gel. Consequently, higher amount of Cu was obtained in the carbonized anodic samples obtained at higher pH. Presence of Na and Cl in the carbonized samples was attributed to the NaCl formed within the gel matrix and detected in the XRD diffractograms. It should be noted that all carbonized samples exhibited a significant presence of nitrogen. This was because chitosan results in nitrogen doped carbon upon carbonization, as reported in previous publi cations [15,37–39]. Similar to carbon, nitrogen also exhibited a decreasing trend with increasing pH. This was expected as both carbon and nitrogen were derived from chitosan.

Both XRD diffractograms and EDX analysis confirmed that the amount of Cu increased in the anodic gel with the increase in the pH of the initial solution from which the chitosan was electro deposited. Our hypothesis is that such phenomenon can be attributed to the chelation behavior between chitosan and Cu^{2+} ions. Chitosan solution exhibits no chelation under high acidic conditions (pH $\leq$ 4), because the $-NH_2$ groups of chitosan get protonated to form NH_3^+. However, when the pH increases to wards neutral values, complexation between $-NH_2$ groups and Cu^{2+} ions starts to form [40–42]. Previous studies already proposed that the complexation of Cu^{2+} with amino group under neutral conditions is carried out in two forms [42,43]. When the pH of chitosan solution is in the range 5–5.8, a complex $[Cu(-NH_2)]^{2+}$ is formed. As the pH increases above 5.8, the second form of complexation $[Cu(-NH_2)_2]^{2+}$ is formed [44,45]. This indicates that, during electrodeposition, the chitosan gel trapped more Cu^{2+} ions in the gel matrix through formation of complexes with increasing pH of the chitosan solution. Furthermore, it also explains why the anodic gels appeared at a pH of 5 or higher. However, more elec trochemical studies are needed to fully understand this mechanism.

2.3. Microstructure of the carbonized anodic gel

Carbonization of the chitosan gels resulted in a porous micro structure (Fig. S4a), which featured mostly large macropores. The pore size distribution was random and irregular. This was mainly attributed to the evaporation of the water from the hydrogel. The carbonized cathodic gel did not feature any Cu particles, as ex pected and shown in Fig. S4b. In contrast, the presence of Cu par ticles was distinctively visible in the scanning electron microscopy (SEM) images of the carbonized anodic gels, as presented in Fig. 3a–c. The SEM measurements have shown a dependency of the size and shape of the Cu particles on the pH of the initial chitosan solution. The shape of the Cu particles for pH 5 and pH 5.5 was spheroidal (see Fig. S5); the particle size distributions of the carbonized gels stemming from chitosan solutions with pH values of 5 and 5.5 are shown in the insets of Fig. 3a and b, respectively. The average size of the Cu particles increased with pH of the initial chitosan solution. The average diameter of the Cu particles ob tained from chitosan solutions with pH values of 5 and pH 5.5 was 3.69 ± 2.67 μm and 6.35 ± 4.68 μm, respectively. Compared to the samples obtained from solutions with pH values of 5 and 5.5, the sample corresponding to the solution with pH 6 exhibited irregular and larger shape of the Cu particles, as shown in Fig. 3c and its inset. We attribute the dependence of the shape and size of the Cu par ticles on pH to the fact that increasing pH results in higher amount of Cu^{2+} in the chitosan hydrogel. The Cu^{2+} ions go through aggre gation and sintering due to close spatial proximity to form sphe roidal particles at higher temperature during carbonization. A higher amount of Cu^{2+} ions with increasing pH of the original chitosan solution resulted in a denser spatial distribution, which yielded larger particles. With further increase in pH, more Cu^{2+} ions get trapped in the hydrogel, causing a dense spatial distribu tion. This might have triggered the formation of the copper parti cles in irregular non spherical shapes. The larger size of the irregular shapes is also evidence of the dense proximity of the Cu^{2+} ions. It should be noted here that the majority of the Cu particles were observed on the surface of the samples; the presence of the Cu particles in the core of the sample was comparatively low (Fig. S6). This might be due to the migration of Cu particles towards the surface during the carbonization process while performing carbonization with metals, reported previously by other re searchers [46–48].

Fig. 3d and e shows the high resolution transmission electron microscopy (HRTEM) images of spots 1 and 2, respectively. Spot 1 represents a site where no Cu particle was present. Spot 2 was chosen on a Cu particle. HRTEM image of Spot 1 exhibited a tur bostratic microstructure of carbon, which is similar to the micro structure observed in the HRTEM of carbonized cathodic gel (Fig. S4d). No graphitized microstructure of carbon was observed here. However, a few layers of graphitized carbon can be seen around the Cu particle, as indicated in Fig. 3e. This indicates that localized graphitization of carbon occurred at the interface of Cu and carbon, however, it was limited to only few layers at the interface. This supports the fact that Cu does not have a strong influence on the graphitization of the carbon, as compared other metals such iron, nickel and cobalt [49–51]. The turbostratic microstructure of the carbon also correlates with the presence of the broad peak around $2\theta \quad 24^{\circ}$ in the XRD diffractograms. The HRTEM image of Spot 2 showed distinct lattice fringes of Cu with a d spacing of 2.14 Å and 1.86 Å, which correspond to the (111) and (200) crystal planes of copper, respectively [52,53].

2.4. Electrical characterization

The electrical conductivity of the carbonized samples was measured using the four point probe method. As the carbonization process resulted in rough, porous and irregular shape carbonized gel samples, it was not feasible to perform the four point probe method on the samples as obtained after the carbonization process. Hence, we prepared circular pellets with a diameter of 10 mm by crushing the carbonized gels into fine powders, followed by mixing with polytetrafluoroethylene (PTFE) additive and compression at high pressure (see Experimental section for details). The four point probe measurements were performed on the circular pellets. As a result, the values obtained from the four point probe tests were not the absolute values for the carbonized samples, rather the mea surements took into account also the PTFE used to form the pellets. However, these measurements can dictate the trend of the elec trical properties of the carbonized samples. The electrical conduc tivity is plotted with respect to the pH of initial chitosan solution in Fig. 4a. One can notice that the standard deviation in the mea surement of electrical conductivity was significantly high. This might be due to the fact that PTFE was used as an additive for the preparation of the pellets. During mixing the carbonized sample with PTFE, a homogeneous mixture was expected, but not observed. We suspect that localized concentration of PTFE as well as Cu particles has occurred. Such localized concentrations might have resulted in significant deviation in the measurement values.

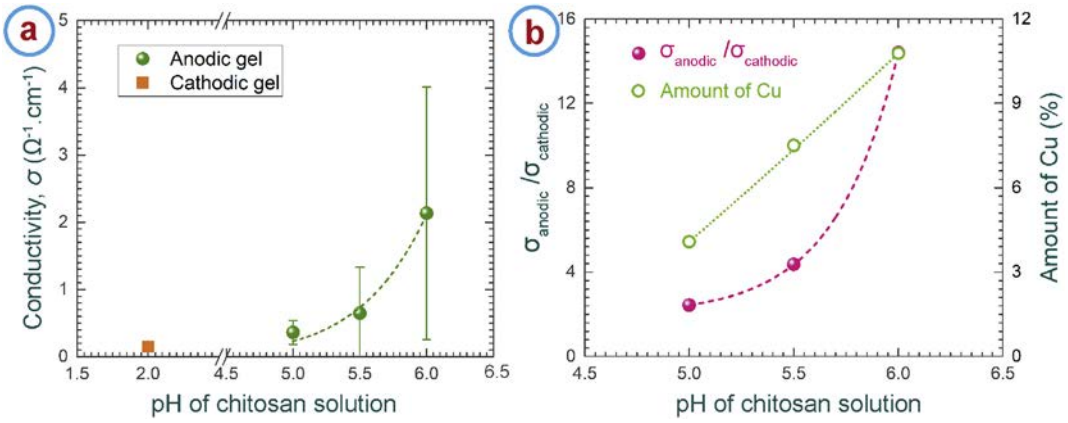

Fig. 4. (a) Effect of pH on the electrical conductivity of the carbonized anodic gels. The conductivity of the carbonized cathodic gel is also plotted for comparison. At least 20 measurements were performed for each data point. The error bar represents standard deviation in measurement. (b) Comparison between the increment in electrical conductivity and amount of Cu in the carbonized samples with the pH of chitosan solution.

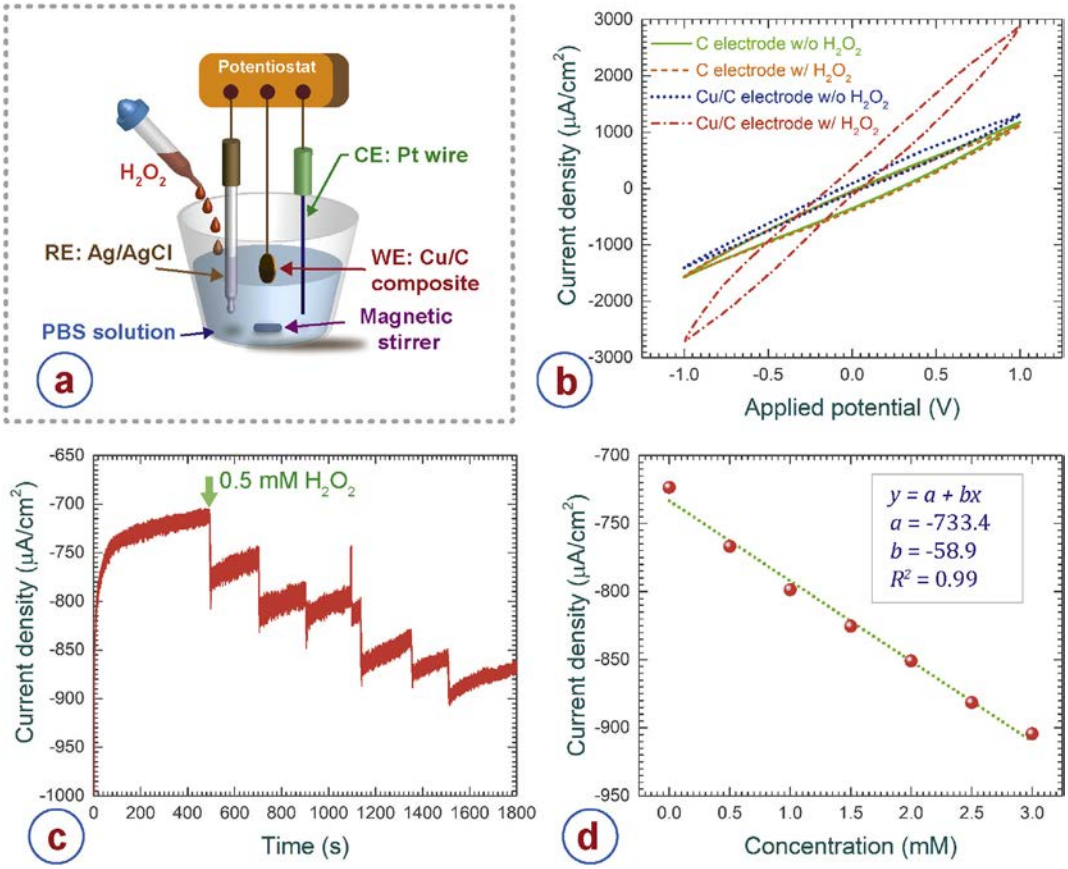

Fig. 5. (a) Schematic illustration of the three-electrode electrochemical set up used for the study of electrochemical sensing of H_2O_2. (b) Cyclic voltammograms (CV) of the cathodic carbon and the anodic copper/carbon samples in the presence and absence of 0.5 mM H_2O_2. 0.02 M PBS solution was used as the electrolyte. (c) Amperometric response of the copper/carbon electrode upon successive addition of 0.5 mM H_2O_2 in the electrolyte. (d) Calibration curve of response current versus concentration of H_2O_2. The anodic copper/carbon sample at pH 6 was used here for the sensing of H_2O_2.

The carbonized anodic samples showed higher conductivity compared to the carbonized cathodic samples. The electrical con ductivity for the cathodic samples was 0.148 ± 0.06/Ω/cm, whereas the electric conductivity for the anodic samples ranged from 0.361 ± 0.179/Ω/cm for the sample obtained from the solution with a pH value of 5, to 2.132 ± 1.87/Ω/cm for the sample obtained from the solution with a pH value of 6. This was expected considering the presence of copper particles in the anodic samples. It was also evident that the electrical conductivity increased within the anodic samples with the increase in the pH of the initial chitosan solution. The sample obtained from the solution with pH 5 exhibited an increase in electrical conductivity of 2.44 fold compared to the cathodic sample, whereas the sample obtained from the solution with pH 6 showed a 14.4 fold increase in electrical conductivity (Fig. 4b). The curve fitting using the average conductivity values within the pH range 5–6 showed that the improvement in the electrical conductivity within this range was exponential. However, such exponential relation might not be true. The pH window is too small, and the number of intervals within the pH window are too few to draw such a conclusion. Nevertheless, the improvement in the conductivity can be attributed to the increase in the amount of Cu in the anodic samples with the increasing pH. We expected that the electrical conductivity would vary linearly in relation to the amount of Cu, which was not the case, as shown in Fig. 4b. Our current hypothesis is that higher amount of Cu resulted in higher proximity among the Cu particles, which enhanced the charge transfer within the carbon/Cu composite. Furthermore, it was seen in the TEM images that localized graphitization occurred at the interface of Cu and carbon. Increased amount of Cu also increased the occurrence of localized graphitization. Graphene has signifi cantly higher electrical conductivity when compared to amorphous carbon [54–56]. Therefore, higher occurrence of localized graphi tization is also supposed to contribute to an increased electrical conductivity of the carbonized anodic gels.

2.5. *Electrochemical sensing of H_2O_2*

We investigated the electrochemical sensing capability of the carbonized anodic samples for the detection of hydrogen peroxide (H_2O_2). The electrochemical measurements were carried out in a typical three electrode electrochemical cell as illustrated in Fig. 5a. 0.02 M phosphate buffered saline (PBS) solution was used as the electrolyte for the electrochemical measurements. We chose the Cu/carbon sample obtained from the precursor chitosan solution with pH 6 for the electrochemical measurements due to the pres ence of the highest amount of copper and therefore the highest electrical conductivity among all samples studied. Further, we compared the electrochemical measurement of the Cu/carbon sample with the carbon sample obtained for cathodic gel. Fig. 5b represents the cyclic voltammograms (CVs) of the cathodic carbon and anodic Cu/carbon samples in the presence and absence of 0.5 mM H_2O_2. It can be seen that the carbon electrode exhibited almost identical CVs in the presence and absence of H_2O_2. The Cu/carbon electrode also exhibited similar CV curve in the absence of

H_2O_2. However, the Cu/carbon displayed a significant increase in current, when H_2O_2 was introduced in the electrolyte. Furthermore, the CV curve was considerably wider than the CV curves for other samples. This is because the Cu particles in Cu/carbon electrode were the electro active sites for the reduction of H_2O_2. In absence of H_2O_2, the Cu in the Cu/carbon electrodes remain as Cu^+, as shown in Eq. (1) [57]. In the presence of H_2O_2, reduction of H_2O_2 occurs at the Cu sites, which results in Cu^{2+} ions (Eq. (2)). Generation of the Cu^{2+} on the Cu/carbon produces more free electrons, which causes higher current in the presence of H_2O_2. Such a reaction at the Cu/carbon electrode in the presence of H_2O_2 thus enables the suc cessful detection of H_2O_2. During a potential sweep of the cyclic voltammetry, the Cu^{2+} ions get reduced to Cu, before it reacts with H_2O_2 again (Eq. (3)) [57,58]. Such reversible reaction keeps the electrode surface active for sensing. It should be noted here that the reactions between Cu and H_2O_2 should result in distinct redox peaks, as reported by other authors [57–60]. However, no distinct redox peak was observed in the CV curve of our Cu/carbon com posite electrode in the presence of H_2O_2. Such behavior can be attributed to the use of the PTFE as the binder material during the electrode preparation. PTFE is a non conductive material, which adds to the impedance of the electrode. We suspect that the impedance of the PTFE might have overshadowed the redox peaks originating from the reactions between Cu and H_2O_2, resulting in an ohmic shape CV curve. A similar phenomenon was reported by Liu et al. where using a non conductive polydopamine film for binding Cu nanoparticles to graphene oxide resulted in a near ohmic shaped CV curve during electrochemical sensing of H_2O_2 [61]. Neverthe less, our electrode was still capable of successful detection of H_2O_2. This was advantageous, because the Cu/carbon electrode did not require any enzyme immobilization on its surface for the detection of H_2O_2, which is needed for majority of the traditional sensor materials and causes difficulties in storage, handling and stability of the sensor material [62,63].

$$Cu + H_2O \rightarrow Cu(OH)_{ads} + H^+ + e^- \quad (1)$$

$$Cu + H_2O_2 \rightarrow Cu_2O + H_2O \quad (2)$$

$$Cu_2O + H_2O + 2e^- \rightarrow 2Cu + 2OH^- \quad (3)$$

We measured the amperometric response of the Cu/carbon electrode upon successive addition of 0.5 mM H_2O_2 in the PBS electrolyte. The amperometric response is presented in Fig. 5c. A considerable change in current was observed upon step wise addition of H_2O_2. A steady state current (95% of the maximum value) was recorded within 3 s, which indicated that the Cu/carbon electrode was capable of fast electron transfer when exposed to H_2O_2. We plotted the calibration curve of the response current with the concentration of H_2O_2 in Fig. 5d. The Cu/carbon electrode exhibited a linear response with the concentration of the H_2O_2. The linear regression equation fitted to the calibration curve was y 733.4 58.9x, with a correlation coefficient of 0.9918. The calibration curve depicted that the sensitivity of the Cu/carbon electrode for sensing of H_2O_2 was 58.9 μA/mM/cm^2. The sensitivity of the electrode material demonstrated in the present work was comparable to that of other non enzymatic amperometric H_2O_2 sensors, as shown in Table S1.

It should be noted that the biosensing measurements were performed using circular pellets prepared from the carbonized anodic gel. The pellets did not feature the inherent porosity of the pristine carbonized samples, and also contained PTFE as binder material. We expect that the pristine Cu/carbon composite material can exhibit higher sensing capabilities due to its purity and porous morphology. However, using the pristine Cu/carbon composite as the working electrode is challenging, because its irregular shape makes it difficult to establish electrical connections within the electrochemical cell. One solution might be integrating the pristine composite with a microelectromechanical system (MEMS) device. Geng et al. showed in their article that it is possible to pattern the anodic chitosan gel on microfabricated copper microelectrodes [19]. Using a similar approach, a MEMS device can potentially be fabricated featuring Cu/carbon composites electrodes, which can facilitate easy electrical connection within an electrochemical cell and enable electrochemical measurements without need for pellet production. Ongoing work includes fabrication of such Cu/carbon based MEMS devices and investigation on their performances in biosensing.

3. Conclusion and outlook

We successfully demonstrated the use of electrodeposition of chitosan on a copper anode as a simple approach for the synthesis of a Cu/carbon composite material. The anodic electrodeposition of chitosan occurred within a small window of pH, ranging from 5 to 6. Electrodeposition within this pH range showed that increasing pH resulted in the generation ofa higher amount of Cu^{2+} ions within the chitosan hydrogel. Carbonization of the Cu/chitosan gel at 900 °C in a nitrogen environment resulted in the synthesis of a Cu/carbon composite. As expected, the amount of Cu in the com posite increased with increasing pH of the chitosan solution used in electrodeposition. The Cu/carbon composite exhibited a 14.4 fold improvement in electrical conductivity compared to chitosan derived carbon material. Furthermore, the composite also exhibited good non enzymatic sensing capability for the detection of H_2O_2. A sensitivity of 58.9 μA/mM cm^2 was achieved for the Cu/carbon material, which is comparable to the other non enzymatic amperometric H_2O_2 biosensors.

Although the current work is focused on the Cu/carbon com posite, we expect that other metal/carbon composite materials can be similarly synthesized using metal ion mediated chitosan elec trodeposition. Previous publications showed that, apart from Cu, chitosan is able to make complexes with other metals too, including with Zn, Fe, Ni and Ag [64–66]. Using such metals as the anode material in the electrodeposition of chitosan is expected to form corresponding metal/chitosan composites, which can be converted to metal/carbon composite through carbonization. However, using each of these metals as electrodes in an electrodeposition needs individual extensive investigation towards optimization of the electrodeposition parameters, the effect of carbonization on the precursor composite materials, and the application of the final composite material. For example, Fe and Ni are known for their superior catalytic properties in graphitization [67,68]. Carboniza tion of Fe or Ni chitosan composites is expected to result in N doped graphene materials, which can be used for high performance energy components and biosensors. Furthermore, smart design and fabrication can enable the integration of different anode materials towards the fabrication of metal/carbon composite based multi material devices, which can be used for multifunctional high per formance devices.

4. Experimental

4.1. Materials

Chitosan (Molecular weight: 190,000–310,000; Product num ber: 448,877), hydrochloric acid (HCl), and sodium hydroxide (NaOH) were purchased from Sigma Aldrich, Germany. Millipore water was used for preparation of all the solutions used in this work.

4.2. Electrodeposition of chitosan

For electrodeposition of chitosan, we first prepared 120 mL of chitosan solution by dispersing 1% w/v (1.2 g) chitosan powder in 115.2 mL of distilled water, followed by adding 4% v/v 2 M HCl (4.8 mL) into the solution with continuous stirring on a magnetic stirrer plate in order to dissolve the chitosan particles. Once all the chitosan was dissolved and a transparent solution was obtained, 1 M NaOH was added to the chitosan solution and stirred for 30 min to obtain a desired pH value of the solution. pH color strips (Sigma Aldrich, product number 109,584) were used to determine the pH value of the solution. Four different chitosan solutions with different pH values were prepared in this work. We used copper foils as both cathode and anode for electrodeposition. Electrode position was performed using a programmable DC power supply (Voltcraft VLP 1602). For all the chitosan solutions, a DC voltage of 25 V was applied to the electrodes during electrodeposition. Each electrodeposition experiment was carried out for 13 min on an electrode surface area of 100 mm^2. After electrodeposition, the hydrogel was scraped off from the electrode surface and immersed in acetone for overnight. Acetone immersion was performed in an attempt to preserve the pore structures during drying, as acetone has significantly lower surface tension than water. After overnight immersion in acetone, the hydrogel was dried at room temperature for a few hours to obtain a xerogel.

4.3. Carbonization

The xerogels were carbonized in a horizontal tube furnace (Carbolite Gero, Carbolite, Germany) under a constant nitrogen flow (0.8 L/min). The heat treatment protocol was adapted from a heating protocol popularly used in the carbon micro electromechanical system (C MEMS) technology to convert a pattern polymer into glassy carbon structures [69–73]. The proto col featured three steps: (i) raising the temperature of the furnace to 900 °C from room temperature with a heating rate of 5 °C/min, (ii) a dwell at 900 °C for 1 h, and (iii) cooling down to room tem perature by natural cooling.

4.4. Characterization

The carbonized samples were characterized for material composition and crystallinity by X ray diffraction (XRD) using a Bruker D8 Advance diffractometer using Cu Kα1,2 radiation (λ 1.5405 Å). We estimated the crystallite size (D) of the Cu in the Cu/carbon composite by using Scherrer equation (Eq. (4)), which correlates D with the wavelength of X ray (λ), the Bragg angle (θ), the half width of the diffraction peak (B), and dimensionless shape factor (k) [74]. When the detailed shape of a crystallite is unknown, as is the case here, a value of k 0.9 is preferred [74,75]. Of note, the crystallite size calculated here is a lower estimate, as any correction for stress/strain and instrumental contributions were not consid ered. Consideration of these contributions in measurement would narrow the line width and thus increase domain size.

$$D \quad \frac{k \cdot \lambda}{B \cdot cos\theta} \tag{4}$$

The microstructure of the carbonization samples was investi gated using a Carl Zeiss AG–SUPRA 60VP scanning electron mi croscope. Energy dispersive X ray (EDX) spectrocopy (Bruker AXS) mounted on the SEM was used to investigate the material composition of the samples. For measurement of electrical sheet resistance of the carbonized samples, we first prepared pellets with a thickness (t) of 185 ± 30 μm. To prepare the pellets, we manually crushed the carbonized samples into powder using a mortar and pestle. 21 g of such powder was homogeneously mixed with 9 g polytetrafluoroethylene (PTFE) binder. This mixture was pressed by 80 ton pressure for 1 min in a universal testing machine to form the pellets. The electrical sheet resistance (Rs) of the pellets were calculated by Eq. (5) by using the resistance (R) values measured using the four point probe method. A Keithley 2,400 source meter was used for recording the resistance value during the four point probe measurement. The conductivity (σ) of the carbonized sam ples was calculated using 6, which relates the conductivity (σ) with the sheet resistance and thickness (t) of the sample.

$$R_s \quad \frac{\pi}{ln2} \cdot R \tag{5}$$

$$\sigma \quad \frac{1}{R_s \cdot t} \tag{6}$$

4.5. H_2O_2 biosensing

For biosensing applications, pellets of carbonized samples were prepared as detailed above. The electrochemical measurement for the biosensing was performed on an Autolab PGSTAT302F (Met rohm AG, Switzerland) electrochemical workstation using a typical three electrode cell. A platinum wire and Ag/AgCl (saturated with aqueous solution of KCl) were used as the counter electrode and the reference electrode respectively. The pellets of carbonized mate rials were used as working electrodes. Cyclic voltammogram measurement and amperometric response were determined by using a 0.02 M PBS (pH 7) as an electrolyte solution. A 0.5 mM H_2O_2 concentration was used to define the catalytic behavior of working electrode. Amperometric response was carried out at 0.80 V po tential at continuous stirring condition.

Authors contribution

Conceptualization – M.I. and V.B.; Experiments and data cura tion – N.A., P.G.W. and M.I.; Formal analysis – M.I., N.A., P.G.W., and V.B.; Project administration – M.I. and V.B.; Supervision – M.I., V.B. and J.G.K.; Writing and revision – M.I., N.A., P.G.W., V.B. and J.G.K. All authors have read and approved the final version of the manuscript.

Data availability

The raw/processed data required to reproduce these findings cannot be shared at this time due to legal or ethical reasons.

Declaration of competing interest

The authors declare that they have no known competing financial interests or personal relationships that could have appeared to influence the work reported in this paper.

Acknowledgement

All the authors thank the Karlsruhe Nano Micro Facility (KNMF) (project number 2019 023 027429), and Prof. Christian Kübel and Dr. Di Wang from the Institute of Nanotechnology (INT), KIT, for facilitating HRTEM characterization. Monsur Islam, Nikhil Arya and Jan G. Korvink acknowledge support from the Deutsche For schungsgemeinschaft (DFG, German Research Foundation) under Germany's Excellence Strategy via the Excellence Cluster 3D Matter Made to Order (EXC 2082/1 390761711). Vlad Badilita

acknowledges support from the DFG through the project number BA 4275/4 1 *Bio PRICE*.

References

[1] J.-B. Raoof, S.R. Hosseini, R. Ojani, S. Mandegarzad, Mof-derived cu/nanoporous carbon composite and its application for electro-catalysis of hydrogen evolution reaction, Energy 90 (2015) 1075 1081.

[2] N. Lingaiah, M.A. Uddin, A. Muto, Y. Sakata, Hydrodechlorination of chlorinated hydrocarbons over metal carbon composite catalysts prepared by a modified carbothermal reduction method, Chem. Commun. (17) (1999) 1657 1658.

[3] A. Bonakdarpour, D. Esau, H. Cheng, A. Wang, E. Gyenge, D.P. Wilkinson, Preparation and electrochemical studies of metal carbon composite catalysts for small-scale electrosynthesis of H2O2, Electrochim. Acta 56 (25) (2011) 9074 9081.

[4] A. Muhulet, F. Miculescu, S.I. Voicu, F. Schütt, V.K. Thakur, Y.K. Mishra, Fundamentals and scopes of doped carbon nanotubes towards energy and biosensing applications, Mater. Today Energy 9 (2018) 154 186.

[5] A. Ahmadivand, B. Gerislioglu, R. Ahuja, Y.K. Mishra, Terahertz plasmonics: the rise of toroidal metadevices towards immunobiosensings, Mater. Today 32 (2020) 108 130.

[6] Y. Pauleau, F. Thiery, Deposition and characterization of nanostructured metal/carbon composite films, Surf. Coating. Technol. 180 (2004) 313 322.

[7] Y. Pauleau, F. Thièry, L. Latrasse, S. Dub, Characteristics of copper/carbon and nickel/carbon composite films produced by microwave plasma-assisted deposition techniques from argon methane gas mixtures, Surf. Coating. Technol. 188 (2004) 484 488.

[8] J. Wang, P.V. Pamidi, D.S. Park, Sol-gel-derived metal-dispersed carbon composite amperometric biosensors, Electroanalysis 9 (1) (1997) 52 55.

[9] L. Zhang, A. Aboagye, A. Kelkar, C. Lai, H. Fong, A review: carbon nanofibers from electrospun polyacrylonitrile and their applications, J. Mater. Sci. 49 (2) (2014) 463 480.

[10] Z. Hasan, D.-W. Cho, I.-H. Nam, C.-M. Chon, H. Song, Preparation of calcined zirconia-carbon composite from metal organic frameworks and its application to adsorption of crystal violet and salicylic acid, Materials 9 (4) (2016) 261.

[11] M. Rinaudo, Chitin and chitosan: properties and applications, Prog. Polym. Sci. 31 (7) (2006) 603 632.

[12] V.K. Thakur, S.I. Voicu, Recent advances in cellulose and chitosan based membranes for water purification: a concise review, Carbohydr. Polym. 146 (2016) 148 165.

[13] J. Deng, M. Li, Y. Wang, Biomass-derived carbon: synthesis and applications in energy storage and conversion, Green Chem. 18 (18) (2016) 4824 4854.

[14] H.-L. Peng, J.-B. Zhang, J.-Y. Zhang, F.-Y. Zhong, P.-K. Wu, K. Huang, J.-P. Fan, F. Liu, Chitosan-derived mesoporous carbon with ultrahigh pore volume for amine impregnation and highly efficient co2 capture, Chem. Eng. J. 359 (2019) 1159 1165.

[15] D. Guo, H. Wei, X. Chen, M. Liu, F. Ding, Z. Yang, Y. Yang, S. Wang, K. Yang, S. Huang, 3d hierarchical nitrogen-doped carbon nanoflower derived from chitosan for efficient electrocatalytic oxygen reduction and high performance lithium sulfur batteries, J. Mater. Chem. 5 (34) (2017) 18193 18206.

[16] S. Fusco, G. Chatzipirpiridis, K.M. Sivaraman, O. Ergeneman, B.J. Nelson, S. Pané, Chitosan electrodeposition for microrobotic drug delivery, Adv. Healthcare Mater. 2 (7) (2013) 1037 1044.

[17] D.W. Lee, H. Lim, H.N. Chong, W.S. Shim, Advances in chitosan material and its hybrid derivatives: a review, Open Biomater. J. 1 (1) (2009).

[18] G.F. Payne, S.R. Raghavan, Chitosan: a soft interconnect for hierarchical assembly of nano-scale components, Soft Matter 3 (5) (2007) 521 527.

[19] Z. Geng, X. Wang, X. Guo, Z. Zhang, Y. Chen, Y. Wang, Electrodeposition of chitosan based on coordination with metal ions in situ-generated by electrochemical oxidation, J. Mater. Chem. B 4 (19) (2016) 3331 3338.

[20] E.R. Mamleyev, S. Heissler, A. Nefedov, P.G. Weidler, N. Nordin, V.V. Kudryashov, K. Lange, N. MacKinnon, S. Sharma, Laser-induced hierarchical carbon patterns on polyimide substrates for flexible urea sensors, NPJ Flexible Electron. 3 (1) (2019) 1 11.

[21] N. Nordin, L. Bordonali, V. Badilita, N. MacKinnon, Spatial and temporal control over multilayer bio-polymer film assembly and composition, Macromol. Biosci. 19 (4) (2019) 1800372.

[22] L.-Q. Wu, H. Yi, S. Li, D. Small, J. Park, G. Rubloff, R. Ghodssi, W. Bentley, G. Payne, Voltage-programmable biofunctionality in mems environments using electrodeposition of a reactive polysaccharide, in: TRANSDUCERS'03. 12th International Conference on Solid-State Sensors, Actuators and Microsystems. Digest of Technical Papers (Cat. No. 03TH8664), vol. 2, IEEE, 2003, pp. 1871 1874.

[23] V. Badilita, M. Powers, S. Koev, H. Yi, G. Payne, R. Ghodssi, Integrated biophotonic hybridization sensor based on chitosan-mediated assembly, in: MEMS/MOEMS Components and their Applications IV, vol. 6464, International Society for Optics and Photonics, 2007, p. 646404.

[24] V. Badilita, I. Shamim, H. Yi, S. Koev, K. Gerasopoulos, R. Ghodssi, Chitosan-mediated biomems platform for optical sensing, in: TRANSDUCERS 2007-2007 International Solid-State Sensors, Actuators and Microsystems Conference, IEEE, 2007, pp. 1095 1098.

[25] H. Ma, J. Sun, Y. Zhang, C. Bian, S. Xia, T. Zhen, Label-free immunosensor based on one-step electrodeposition of chitosan-gold nanoparticles biocompatible film on au microelectrode for determination of aflatoxin b1 in maize, Biosens. Bioelectron. 80 (2016) 222 229.

[26] X. Pang, I. Zhitomirsky, Electrodeposition of hydroxyapatite silver chitosan nanocomposite coatings, Surf. Coating. Technol. 202 (16) (2008) 3815 3821.

[27] X. Li, J. Yao, F. Liu, H. He, M. Zhou, N. Mao, P. Xiao, Y. Zhang, Nickel/copper nanoparticles modified tio2 nanotubes for non-enzymatic glucose biosensors, Sensor. Actuator. B Chem. 181 (2013) 501 508.

[28] P.A. Fiorito, C.M. Brett, S.I.C. de Torresi, Polypyrrole/copper hexacyanoferrate hybrid as redox mediator for glucose biosensors, Talanta 69 (2) (2006) 403 408.

[29] S. Koev, P. Dykstra, X. Luo, G. Rubloff, W. Bentley, G. Payne, R. Ghodssi, Chitosan: an integrative biomaterial for lab-on-a-chip devices, Lab Chip 10 (22) (2010) 3026 3042.

[30] Y. Liu, E. Kim, R. Ghodssi, G.W. Rubloff, J.N. Culver, W.E. Bentley, G.F. Payne, Biofabrication to build the biology device interface, Biofabrication 2 (2) (2010), 022002.

[31] K.M. Gray, B.D. Liba, Y. Wang, Y. Cheng, G.W. Rubloff, W.E. Bentley, A. Montembault, I. Royaud, L. David, G.F. Payne, Electrodeposition of a biopolymeric hydrogel: potential for one-step protein electroaddressing, Biomacromolecules 13 (4) (2012) 1181 1189.

[32] S.-T. Lee, F.-L. Mi, Y.-J. Shen, S.-S. Shyu, Equilibrium and kinetic studies of copper (ii) ion uptake by chitosan-tripolyphosphate chelating resin, Polymer 42 (5) (2001) 1879 1892.

[33] Y. Li, L. Mu, Y.-S. Hu, H. Li, L. Chen, X. Huang, Pitch-derived amorphous carbon as high performance anode for sodium-ion batteries, Energy Storage Mater 2 (2016) 139 145.

[34] A. Sharma, T. Kyotani, A. Tomita, Comparison of structural parameters of pf carbon from xrd and hrtem techniques, Carbon 38 (14) (2000) 1977 1984.

[35] I. Wróbel-Iwaniec, N. Díez, G. Gryglewicz, Chitosan-based highly activated carbons for hydrogen storage, Int. J. Hydrogen Energy 40 (17) (2015) 5788 5796.

[36] A. Olejniczak, M. Lezanska, J. Wloch, A. Kucinska, J.P. Lukaszewicz, Novel nitrogen-containing mesoporous carbons prepared from chitosan, J. Mater. Chem. 1 (31) (2013) 8961 8967.

[37] T. Wu, G. Wang, X. Zhang, C. Chen, Y. Zhang, H. Zhao, Transforming chitosan into n-doped graphitic carbon electrocatalysts, Chem. Commun. 51 (7) (2015) 1334 1337.

[38] L. Wang, B. Li, F. Xu, X. Shi, D. Feng, D. Wei, Y. Li, Y. Feng, Y. Wang, D. Jia, et al., High-yield synthesis of strong photoluminescent n-doped carbon nanodots derived from hydrosoluble chitosan for mercury ion sensing via smartphone app, Biosens. Bioelectron. 79 (2016) 1 8.

[39] Y.-Y. Wang, B.-H. Hou, H.-Y. Lü, F. Wan, J. Wang, X.-L. Wu, Porous n-doped carbon material derived from prolific chitosan biomass as a high-performance electrode for energy storage, RSC Adv. 5 (118) (2015) 97427 97434.

[40] R.-S. Juang, F.-C. Wu, R.-L. Tseng, Adsorption removal of copper (ii) using chitosan from simulated rinse solutions containing chelating agents, Water Res. 33 (10) (1999) 2403 2409.

[41] D. Liu, Z. Li, Y. Zhu, Z. Li, R. Kumar, Recycled chitosan nanofibril as an effective cu (ii), pb (ii) and cd (ii) ionic chelating agent: adsorption and desorption performance, Carbohydr. Polym. 111 (2014) 469 476.

[42] E. Guibal, Interactions of metal ions with chitosan-based sorbents: a review, Separ. Purif. Technol. 38 (1) (2004) 43 74.

[43] M. Rhazi, J. Desbrieres, A. Tolaimate, M. Rinaudo, P. Vottero, A. Alagui, Contribution to the study of the complexation of copper by chitosan and oligomers, Polymer 43 (4) (2002) 1267 1276.

[44] A. Domard, pH and cd measurements on a fully deacetylated chitosan: application to CuII polymer interactions, Int. J. Biol. Macromol. 9 (2) (1987) 98 104.

[45] K. Kurita, T. Sannan, Y. Iwakura, Studies on chitin. vi. binding of metal cations, J. Appl. Polym. Sci. 23 (2) (1979) 511 515.

[46] N. Yoshizawa, H. Hatori, Y. Soneda, Y. Hanzawa, K. Kaneko, M.S. Dresselhaus, Structure and electrochemical properties of carbon aerogels polymerized in the presence of Cu2+, J. Non-Cryst. Solids 330 (1 3) (2003) 99 105.

[47] J.A. Lie, M.-B. Hagg, Carbon membranes from cellulose and metal loaded cellulose, Carbon 43 (12) (2005) 2600 2607.

[48] M. Islam, D. Keck, R. Martinez-Duarte, Architected tungsten carbide electrodes using origami techniques, Adv. Eng. Mater. 21 (12) (2019), 1900290.

[49] A. Oya, S. Otani, Catalytic graphitization of carbons by various metals, Carbon 17 (2) (1979) 131 137.

[50] R. Sinclair, T. Itoh, R. Chin, In situ tem studies of metal carbon reactions, Microsc. Microanal. 8 (4) (2002) 288 304.

[51] E. Thompson, A. Danks, L. Bourgeois, Z. Schnepp, Iron-catalyzed graphitization of biomass, Green Chem. 17 (1) (2015) 551 556.

[52] I. Lisiecki, A. Filankembo, H. Sack-Kongehl, K. Weiss, M.-P. Pileni, J. Urban, Structural investigations of copper nanorods by high-resolution tem, Phys. Rev. B 61 (7) (2000) 4968.

[53] A.K. Chawla, R. Chandra, Synthesis and structural characterization of nanostructured copper, J. Nanoparticle Res. 11 (2) (2009) 297 302.
[54] H. Riley, Amorphous carbon and graphite, Q. Rev. Chem. Soc. 1 (1) (1947) 59 72.
[55] H. Fredriksson, Nanostructures of Graphite and Amorphous Carbon-Fabrication and Properties, Chalmers University of Technology, 2009.
[56] S. Rattanaweeranon, P. Limsuwan, V. Thongpool, V. Piriyawong, P. Asanithi, Influence of bulk graphite density on electrical conductivity, Procedia Eng. 32 (2012) 1100 1106.
[57] A.A. Ensafi, M.M. Abarghoui, B. Rezaei, Electrochemical determination of hydrogen peroxide using copper/porous silicon based non-enzymatic sensor, Sensor. Actuator. B Chem. 196 (2014) 398 405.
[58] M. Somasundrum, K. Kirtikara, M. Tanticharoen, Amperometric determination of hydrogen peroxide by direct and catalytic reduction at a copper electrode, Anal. Chim. Acta 319 (1 2) (1996) 59 70.
[59] A.A. Ensafi, N. Zandi-Atashbar, M. Ghiaci, M. Taghizadeh, B. Rezaei, Synthesis of new copper nanoparticle-decorated anchored type ligands: applications as non-enzymatic electrochemical sensors for hydrogen peroxide, Mater. Sci. Eng. C 47 (2015) 290 297.
[60] T. Selvaraju, R. Ramaraj, Electrocatalytic reduction of hydrogen peroxide at nanostructured copper modified electrode, J. Appl. Electrochem. 39 (3) (2009) 321 327.
[61] Y. Liu, Y. Han, R. Chen, H. Zhang, S. Liu, F. Liang, In situ immobilization of copper nanoparticles on polydopamine coated graphene oxide for h2o2 determination, PloS One 11 (7) (2016), e0157926.
[62] C. Revathi, et al., Enzymatic and nonenzymatic electrochemical biosensors, in: Fundamentals and Sensing Applications of 2D Materials, Elsevier, 2019, pp. 259 300.
[63] W.-C. Lee, K.-B. Kim, N. Gurudatt, K.K. Hussain, C.S. Choi, D.-S. Park, Y.-B. Shim, Comparison of enzymatic and non-enzymatic glucose sensors based on hierarchical au-ni alloy with conductive polymer, Biosens. Bioelectron. 130 (2019) 48 54.
[64] X. Wang, Y. Du, L. Fan, H. Liu, Y. Hu, Chitosan-metal complexes as antimicrobial agent: synthesis, characterization and structure-activity study, Polym. Bull. 55 (1 2) (2005) 105 113.
[65] A.A. Emara, M.A. Tawab, M. El-Ghamry, M.Z. Elsabee, Metal uptake by chitosan derivatives and structure studies of the polymer metal complexes, Carbohydr. Polym. 83 (1) (2011) 192 202.
[66] D.K. Božanić, L.V. Trandafilović, A.S. Luyt, V. Djoković, 'Green' synthesis and optical properties of silver chitosan complexes and nanocomposites, React. Funct. Polym. 70 (11) (2010) 869 873.
[67] W. Kiciński, M. Norek, M. Bystrzejewski, Monolithic porous graphitic carbons obtained through catalytic graphitization of carbon xerogels, J. Phys. Chem. Solid. 74 (1) (2013) 101 109.
[68] F. Maldonado-Hódar, C. Moreno-Castilla, J. Rivera-Utrilla, Y. Hanzawa, Y. Yamada, Catalytic graphitization of carbon aerogels by transition metals, Langmuir 16 (9) (2000) 4367 4373.
[69] M. Islam, A.D. Lantada, M.R. Gómez, D. Mager, J.G. Korvink, Microarchitectured carbon structures as innovative tissue engineering scaffolds, Adv. Eng. Mater. (2020), 2000083, https://doi.org/10.1002/adem.202000083.
[70] M. Islam, D. Keck, J. Gilmore, R. Martinez-Duarte, Characterization of the dielectrophoretic response of different candida strains using 3d carbon microelectrodes, Micromachines 11 (3) (2020) 255.
[71] M. Islam, J. Flach, R. Martinez-Duarte, Carbon origami: a method to fabricate lightweight carbon cellular materials, Carbon 133 (2018) 140 149.
[72] M. Elitas, Y. Yildizhan, M. Islam, R. Martinez-Duarte, D. Ozkazanc, Dielectrophoretic characterization and separation of monocytes and macrophages using 3d carbon-electrodes, Electrophoresis 40 (2) (2019) 315 321.
[73] R. Natu, M. Islam, J. Gilmore, R. Martinez-Duarte, Shrinkage of su-8 microstructures during carbonization, J. Anal. Appl. Pyrol. 131 (2018) 17 27.
[74] U. Holzwarth, N. Gibson, The scherrer equation versus the' debye-scherrer equation', Nat. Nanotechnol. 6 (9) (2011), 534 534.
[75] V. Uvarov, I. Popov, Metrological characterization of x-ray diffraction methods for determination of crystallite size in nano-scale materials, Mater. Char. 58 (10) (2007) 883 891.